

1 **A highly contiguous, scaffold-level nuclear genome assembly for the Fever tree (*Cinchona*
2 *pubescens* Vahl) as a novel resource for research in the Rubiaceae**

3

4 Nataly Allasi Canales^{1,2*}, Oscar A. Pérez-Escobar^{2,9*}, Robyn F. Powell², Mats Töpel³,
5 Catherine Kidner⁴, Mark Nesbitt², Carla Maldonado⁵, Christopher J. Barnes⁶, Nina Rønsted^{1,7},
6 Natalia A. S. Przelomska², Ilia J. Leitch²⁺, Alexandre Antonelli^{2,9,10+}

7

8 ¹Natural History Museum of Denmark, University of Copenhagen, Denmark.

9 ²Royal Botanic Gardens, Kew, London, UK.

10 ³University of Gothenburg, Department of Marine Sciences, Sweden.

11 ⁴Royal Botanic Garden Edinburgh, Edinburgh, UK

12 ⁵Herbario Nacional de Bolivia, Instituto de Ecología, Universidad Mayor de San Andrés, La
13 Paz, Bolivia

14 ⁶The Globe Institute, University of Copenhagen, Denmark

15 ⁷National Tropical Botanical Garden, Kalaheo, Hawaii, USA

16 ⁹Gothenburg Global Biodiversity Centre, Sweden.

17 ¹⁰Department of Plant Sciences, University of Oxford, Oxford, UK.

18

19

20

21

22 *These authors contributed equally to the study.

23 ⁺Joint senior authors

24

25

26 **Abstract**

27
28 **Background:** The Andean Fever tree (*Cinchona* L.; Rubiaceae) is the iconic source of
29 bioactive quinine alkaloids, which have been vital to treating malaria for centuries. *C.*
30 *pubescens* Vahl, in particular, has been an essential source of income for several countries
31 within its native range in north-western South America. However, an absence of available
32 genomic resources is essential for placing the *Cinchona* species within the tree of life and
33 setting the foundation for exploring the evolution and biosynthesis of quinine alkaloids.

34

35 **Findings:** We address this gap by providing the first highly contiguous and annotated nuclear
36 and organelle genome assemblies for *C. pubescens*. Using a combination of ~120 Gb of long
37 sequencing reads derived from the Oxford Nanopore PromethION platform and 142 Gb of
38 short-read Illumina data. Our nuclear genome assembly comprises 603 scaffolds comprising a
39 total length of 904 Mb, and the completeness represents ~85% of the genome size (1.1 Gb/1C).
40 This draft genome sequence was complemented by annotating 72,305 CDSs using a
41 combination of *de novo* and reference-based transcriptome assemblies. Completeness analysis
42 revealed that our assembly is moderately complete, displaying 83% of the BUSCO gene set
43 and a small fraction of genes (4.6%) classified as fragmented. Additionally, we report *C.*
44 *pubescens* plastome with a length of ~157 Kb and a GC content of 37.74%. We demonstrate
45 the utility of these novel genomic resources by placing *C. pubescens* in the Gentianales order
46 using additional plastid and nuclear datasets.

47

48 **Conclusions:** Our study provides the first genomic resource for *C. pubescens*, thus opening
49 new research avenues, including the provision of crucial genetic resources for analysis of
50 alkaloid biosynthesis in the Fever tree.

51

52 **Keywords:** Oxford Nanopore Technologies, Rubiaceae, RNA-seq, whole-genome sequencing,

53 *Cinchona*, quinine

54

55 **Data Description**

56 **1.1 Background**

57 The Andes biodiversity hotspot hosts over 28,000 species [1], of which 3,805 benefit
58 humanity [2]; unfortunately, nuclear genomic resources are only available for a limited number
59 of such diversity (179 spp – Genomes NCBI database accessed on 26 May 2022). The fever
60 tree (*Cinchona* L., Rubiaceae) is a genus comprising 24 species native to the Eastern slopes of
61 the Andes mountain range in South America ([3,4]; Fig. 1) and one of the most economically
62 important genera in the family, second only to coffee [5]. The genus is widely known as the
63 source of at least 35 quinine alkaloids (quinolines), which alleviate the fever symptoms
64 associated with malaria [6]. As such, fever trees have played a crucial role in the economies
65 and livelihoods of people worldwide for centuries [7,8].

66 Despite this genus's tremendous historical and economic importance, DNA sequence

67 datasets for *Cinchona* are relatively meagre, limited to 252 DNA Sanger sequences available
68 in the NCBI repository (accessed on May 17, 2021; [9]). More importantly, no nuclear and
69 organellar reference genomes exist for any species of the genus. As such, important
70 fundamental and applied questions – such as the mode and tempo of evolution of the fever tree
71 or the genetic pathways responsible for quinine alkaloid production – remain elusive. Previous
72 phylogenetic studies of the Rubiaceae family, specifically of the Cinchonoideae subfamily
73 where the Cinchoneae tribe is, are based on just a handful of nuclear (ITS) and plastid (*matK*,
74 *rcbL*, *rps16*, *trnL-F*) data sets. They show an unresolved polytomy between the tribes and the
75 seven genera of the Cinchoneae tribe that have so far been included in more specific studies
76 [10,11] (including the genus *Cinchona*, which shows very unclear relationships). Furthermore,
77 studies that examine the relationships between species of this genus are equally scarce [7,8]. A

78 recent genome-wide phylogenetic tree for the order Gentianales [12] provided strong support
79 for *C. pubescens* as a sister to *Isertia hypoleuca*, but the sampling was exclusively at the genus
80 level and therefore did not include any other species of *Cinchona* nor other genera in tribe
81 Cinchoneae.

82 The production of alkaloids is highest in *C. calisaya*, also known as yellow bark
83 [13][14]. However, several species in the genus have historically been harvested to provide
84 sources of quinine alkaloids, one of the most traded natural products, resulting in significant
85 reductions in their natural ranges and population size [15,16]. Among them, *C. pubescens* or
86 red Cinchona bark is now widely cultivated throughout the tropics, with some instances where
87 the species has escaped cultivation and become invasive [17]. Extensive research on the
88 structure, abundance, and chemical composition of quinine alkaloids in *Cinchona* has been
89 conducted [18], revealing the further potential for novel drug discovery. However, the identity
90 of the genes involved in the synthetic pathway of quinine alkaloids remains elusive.

91 Nuclear genome assemblies are critical to our understanding of the origin and
92 domestication of useful plants and are a cornerstone resource for breeders [19–21]. Here, we
93 present the first high-quality draft nuclear and plastid genomes of *C. pubescens*, which is
94 characterised by having a genome size of 1.1 Gb (1C, this study) and a chromosome number
95 of 2n=34. The assemblies were generated using a combination of extensive long-read Nanopore
96 (~218x) and short-read Illumina paired-end read datasets (~300x) jointly with state-of-the-art
97 genome assemblers, resulting in a reference genome for which contiguity and quality are
98 comparable to, or even higher [22] than in the three previously published genome assemblies
99 in Rubiaceae, namely for *Chiococca alba* [22], *Coffea canephora* [23], and *Coffea arabica*
100 [24]. The plastid genome from short-reads of *C. pubescens* had a length of 156,985 bp and a
101 GC content of 37.74%, very similar to other Rubiaceae plastid genomes [22,25]. Lastly, we

102 demonstrate the utility and reliability of our resources by constructing nuclear and plastid
103 phylogenomic frameworks of *C. pubescens*.

104

105 **1.2 Sampling and genomic DNA and RNA sequencing**

106 We sampled leaves from a single *Cinchona pubescens* individual propagated
107 vegetatively from a tree collected in Tanzania in 1977 and cultivated in the Temperate House
108 of the Royal Botanic Gardens, Kew (RBG Kew), UK (Accession Number 1977-69; a voucher
109 was also prepared which is deposited in the RBG Kew herbarium [K]). DNA was extracted
110 from fresh tissue using two different protocols to produce paired-end Illumina and native
111 Nanopore libraries. For Illumina DNA library preparations, we used 1000 mg of starting
112 material that was first frozen with liquid nitrogen and subsequently ground in a mortar. The
113 Qiagen DNeasy (Qiagen, Denmark) plant kit was used to extract DNA from the ground tissue,
114 following the manufacturer's protocol. We built the libraries using the Illumina TruSeq PCR-
115 free library (NEX, Ipswich, MA, USA) following the manufacturer's protocol, by first
116 assessing the DNA quantity and quality using a Nanodrop fluorometer (Thermo Scientific,
117 Denmark) and then fragmenting oligonucleotide strands through ultrasonic oscillation using a
118 Covaris ME220 (Massachusetts, USA) device to yield fragments with an average length of 350
119 bp. Then we sequenced the paired-end 150 bp libraries using the HiSeq X Ten chemistry. For
120 transcriptome library preparations, total RNA was extracted from 1000 mg of frozen-ground
121 leaf, young bract, mature bract, flower anthesis, flower bud (older), flower bud (young), leaf
122 bud and young leaf tissue using the TRIzol reagent (Thermo Fisher Scientific, Denmark)
123 following the manufacturer's protocol. Illumina library preparation and sequencing were
124 conducted by Genewiz GmbH (Leipzig, Germany).

125 The Nanopore sequencing data were generated and base called as part of Oxford
126 Nanopore's London Calling 2019 conference [26]. For Nanopore library preparation, 1000 mg

127 of leaf tissue was frozen and ground with a mortar and pestle. The lysis was carried with
128 Carlson lysis buffer (100 mM Tris-HCl, pH 9.5, 2% CTAB, 1.4 M NaCl, 1% PEG 8000, 20
129 mM EDTA) supplemented with β -mercaptoethanol. The sample was extracted with chloroform
130 and precipitated with isopropanol. Finally, it was purified using the QIAGEN Blood and Cell
131 Culture DNA Maxi Kit (Qiagen, UK). Size selection was performed using the Circulomics
132 Short Read Eliminator kit (Circulomics, MD, USA) to deplete fragments below 10 kb. DNA
133 libraries were prepared using the ONT Ligation Sequencing Kit (SQK-LSK109, Oxford
134 Nanopore Technologies, UK). During sequencing on the PromethION platform, re-loads were
135 performed when required. Though yield was slightly lower in sequencing for these re-loaded
136 samples (over 50 Gb in 24 hours), the read N50 was over 48 kb (up from 28 kb without size
137 selection).

138

139 **1.3 Estimation of genome size**

140 To accurately determine the genome size of *C. pubescens*, we followed the one-step flow
141 cytometry procedure [27], with modifications as described in Pellicer et al. [28]. Freshly
142 collected tissue from the same individual sampled for DNA and RNA sequencing was
143 measured together with *Oryza sativa* L. ‘IR-36’ as the calibration standard using general-
144 purpose buffer” (GPB) [29] supplemented with 3% PVP-40 and β -mercaptoethanol [28]. The
145 samples were analysed on a Partec Cyflow SL3 flow cytometer (Partec GmbH, Münster,
146 Germany) fitted with a 100 mW green solid-state laser (532 nm, Cobolt Samba, Solna,
147 Sweden). Three replicates were prepared and the output histograms were analysed using the
148 FlowMax software v.2.4 (Partec GmbH, Münster, Germany). The 1C-value of *C. pubescens*
149 was calculated as (Mean peak position of *C. pubescens*/Mean peak position of *O. sativa*) \times 0.49
150 Gb (=1C value of *O. sativa*) [30] and resulted in a 1C-value of 1.1 Gb. Additionally, using the
151 full Illumina short-read dataset, we additionally implemented a k-mer counting method to

152 characterise the genome in Jellyfish v.2.2.10 [31] setting a kmer size of 21. We used
153 GenomeScope to visualise the kmer plot [32]. However, we did not deem the kmer counting
154 method sufficiently accurate for genome size estimation but reported the estimated genome-
155 wide heterozygosity rates output by GenomeScope as 0.869-0.889%.

156 **1.4 Short read data processing of the chloroplast genome assembly**

157 Sequencing of the DNA Illumina library generated 428M paired-end reads,
158 representing 128.4 Gb of raw data. RNA sequencing produced 385M paired-end reads,
159 representing 115.5 Gb (Table 1). The quality of the raw reads was assessed using the FastQC
160 software [33], and quality trimming was conducted using the software AdapterRemoval2
161 v.2.3.1 [34]. Here, bases with Phred score quality <30 and read lengths <50 bp were removed
162 together with adapter sequences. The final short-read dataset was 131 Gb and contained
163 384,626,011 paired reads, which corresponds to an estimated 464.8x coverage (based on the
164 genome size of 1.1 Gb/1C, see *Estimation of genome size*).

165 The plastid genome of *C. pubescens* was assembled using only short reads, as there
166 were some discrepancies using the hybrid dataset. The toolkit GetOrganelle v.1.7.5, was used
167 with the parameters suggested for assembling plastid genomes in Embryophyta (i.e.,
168 parameters -R 15, -k 21,45,65,85,105, -F embplant_pt). GetOrganelle produced a single linear
169 representation of the *C. pubescens* plastid genome, with a length of 156,985 bp (Fig. 2) and a
170 GC content of 37.74%. These values are very similar to those reported for the *Coffea arabica*
171 plastid genome, which is reported to be 155,189 bp in length and has a GC content of 37.4%
172 [25].

173 We annotated the plastid genome assembly of *C. pubescens* in CHLOROBOX [35],
174 which implements GeSeq [36], tRNAscan-SE v2.0.5 [37], and ARAGORN v1.2.38 [38].
175 CHLOROBOX annotations indicated that the *C. pubescens* genome has the typical angiosperm
176 quadripartite structure, i.e., Inverted Repeat (IRa and IRb) (each 27,502 bp long), the Small

177 Single Copy (SSC) region (18,051 bp), and the Large Single Copy (LSC) region (83,930 bp).
178 We predicted 128 genes, of which 34-37 were tRNA (tRNAscan-SE and ARAGORN,
179 respectively), 81 CDSs, and four ribosomal RNAs (rRNAs). The junction between SSC-IRa
180 and LSC-IRa contains the *ycf1* pseudogene and *rps3* gene, respectively. Similarly, the junction
181 between IRb-SSC and LSC-IRb contains the *ycf1* pseudogene and *rsp3* gene, respectively
182 (Supp. Fig. 1). The final structural features of the *C. pubescens* plastid genome were generated
183 using OGDRAW v. 1.3.1 [39] (Fig. 2) and edited manually. Finally, the quality of the plastid
184 genome assembly was estimated by mapping the Illumina DNA short reads to the newly
185 assembled genome using the bam pipeline in Paleomix [40], where we used BWA [41] for
186 alignment, specifying the backtrack algorithm, and filtering minimum quality equal to zero to
187 maximise recovery. After PCR duplicate filtering, the coverage of unique hits was 7,960x.

188

189 **1.5 Long-read nuclear genome assembly, quality assessment and ploidy levels**

190 The quality and quantity of the PromethION sequencing output conducted across four
191 flow cells were evaluated in NanoPlot v.1.82 [42] independently for each flow cell, using as
192 input the sequencing summary report produced by Guppy v3.0.3. Overall, the average read
193 length, Phred score quality and N50 following base calling with Guppy v3.0.3, and the High
194 Accuracy model reached values of ~19,000 bp, 9, and ~46,000 bp, for mean read length, mean
195 read quality and read length N50, respectively (Supp. Tab. 1). A total of 13,252,640 quality-
196 passed reads were produced, representing ~262 Gb and providing a theoretical genome
197 coverage of ~218x. To assemble the raw Nanopore reads into scaffolds, we first corrected and
198 trimmed the quality-passed reads using the software CANU v.1.9 [43] in correction and
199 trimming mode with the following parameters: *genomeSize* = 1.1g, *-nanopore-raw*. This step
200 generated a total of 1,265,511 reads, representing c. 89 Gb, or a theoretical genome coverage
201 of 74x. Next, the corrected/trimmed reads were used as input into SMARTdenovo v.1.0 [44],

202 using the following parameters: *-c 1* (generate consensus mode), *-k 16* (k-mer length) and *-J*
203 5000 (minimum read length). This step produced an assembly composed of 603 scaffolds with
204 an N50 of 2,783,363 bp, representing ~904 Mb (~82% of the genome size; Tab. 1). Lastly, a
205 round of scaffold correction was implemented in RACON v.1.4.3 [45] using as input the
206 corrected Nanopore reads generated by CANU and an alignment SAM file produced by
207 mapping the trimmed DNA Illumina reads against the assembly produced by SMARTdenovo.
208 The alignment file was produced by Minimap2 v.2.18 [46] using the “accurate genomic read
209 mapping” settings designed to map short-read Illumina data (flag *-ax*). RACON was executed
210 using an error threshold of 0.3 (*-e* flag), a quality threshold of 10 (*-q*), and a window length of
211 500 (*-w*). The corrected assembly differed little compared with the raw assembly produced by
212 SMARTdenovo (Tab. 1).

213 We followed a two-pronged approach to assess the quality of our corrected nuclear
214 genome assembly by i) evaluating the proportion of Illumina reads that mapped against our
215 new genome assembly using as input the alignment file (SAM) generated by Minimap2 and
216 computing coverage and mean depth values per scaffold, as implemented in the function *view*
217 (flag *-F 260*) of the software Samtools v1.12 [47]; and ii) estimating the completeness of the
218 genome as implemented in the software BUSCO v.5.2 and using the *viridiplantae_odb10* [48].
219 A total of 827,098,761 reads were mapped against the corrected genome assembly,
220 representing 99% of the trimmed reads used as input (241,498,983). Mean coverage and read
221 depth ranged from 26-48x. The genome completeness analysis recovered a total of 92.4%
222 conserved eudicot genes, of which 87.5% were single copy, 4.9% duplicated, and 5.6%
223 fragmented. The remaining BUSCO genes were labelled as missing (2%). Taken together, our
224 results suggest that our nuclear genome assembly presents high contiguity and quality with
225 high completeness.

226 Lastly, to evaluate the ploidy levels of *C. pubescens* through the newly assembled
227 genome, we computed allele frequencies from reads mapped against two scaffolds, “utg 230”
228 and “utg2” derived from our genome assembly, covering 9,568,509 bp (~106x coverage) and
229 14,628,764 bp (~103x coverage), respectively. The reads were obtained from the mapping
230 procedure conducted to assess the quality of the corrected nuclear genome assembly (see
231 above). We relied on the software ploidyNGS to compute allele frequencies [49], using the -g
232 option (i.e. guess ploidy levels), a maximum read depth of 100 option (-d 100) and a maximum
233 allele frequency of 0.95 (-m 0.95). Our analysis revealed that the genome of *C. pubescens* is
234 diploid (Fig. 3) as inferred by the comparison of Kolmogorov-Smirnoff distances between the
235 allele frequencies computed from our read mappings and those derived from simulated data
236 [49].

237

238 **1.6 Transcriptome assembly, candidate gene annotation, and quality assessment**

239 To produce a comprehensive database of assembled transcripts, we generated
240 reference-based and *de-novo* assemblies with the Trinity toolkit v. 2.8 [50] using the trimmed
241 RNA-seq data. The reference-based assembly was conducted using as input the aligned RNA-
242 seq trimmed reads against our new reference genome as produced by aligner STAR v.2.9 [51]
243 with default settings, and a maximum intron length of 57,000 as estimated for *Arabidopsis*
244 *thaliana* (flag --genome_guided_max_intron). The *de-novo* transcriptome assemblies were also
245 produced using the default settings of Trinity and the trimmed RNA-seq reads as input. A
246 comprehensive database of *de-novo* and reference-based assembled transcriptomes was
247 compiled with the software PASA v.2.0.2 [52], using the following parameters: --min_per_ID
248 95, and --min_per_aligned 30.

249 To assess the completeness of the *de-novo* transcriptome assembly, we used BUSCO
250 v.5.12 and the representative plant set viridiplantae_odb10, which currently includes 72

251 species, of which 56 are angiosperms. Our assembled transcriptome captured 92.7% (394/425)
252 of the BUSCO set as complete genes, of the remainder, 3.1% of the genes were fragmented,
253 and 4.2% were missing.

254 We predicted the structure and identity of the genes in the nuclear genome using the
255 comprehensive transcriptome assembly compiled with PASA. For this purpose, we used
256 AUGUSTUS v3.3.3 [53] for a combination approach of *ab initio* and transcript evidence-based
257 on RNA-seq data. As AUGUSTUS considered the transcripts' evidence as Expressed Sequence
258 Tag (EST), we first generated hints from the transcriptome data by aligning the transcripts to
259 the genome using BLAT v 3.5 [54]. Then, we set the hint parameters to rely on the hints and
260 anchor the gene structure. We predicted 72,305 CDSs using the hints and tomato (*Solanum*
261 *lycopersicum* L.) as the reference species. The completeness of the CDSs was estimated using
262 BUSCO v.5.12 and *vidiriplantae* odb10 [48] as reference: 68.4% represented complete
263 BUSCOs, 63.5% were single-copy, 26% were fragmented and 5.6% were missing. We
264 summarized the metrics of the CDSs statistics with GenomeQC (Table 1) [55]

265 **1.7 Nuclear and plastid phylogenomics of *Cinchona***

266 We verified the nuclear genome's phylogenetic placement using the reference
267 sequences of the 353 low-copy nuclear genes that are conserved across angiosperms from the
268 Plant and Fungal Trees of Life project [56]. Here, we sampled the gene sequences for the 18
269 taxa from the Gentianales, which included another *C. pubescens* from that study (Supp. Tab.
270 2) that are publicly available in the Tree of Life Explorer [57] hosted by the Royal Botanic
271 Gardens, Kew. To include the *C. pubescens* of this study in the analysis of the 353 low copy
272 nuclear genes of selected Gentianales, we then retrieved these genes from our RNA-seq data
273 using the pipeline HybPiper v.1.3.1 [58]. Given the abundance of RNA-seq read data, to render
274 the gene retrieval tractable, as input for HybPiper we used a subsample of the trimmed read
275 data, as implemented in the software seqtk [59]. The gene sequences produced by HybPiper

276 were aligned with the data for 19 selected Gentianales species using MAFFT v7.453 [60] and
277 then they were concatenated into a supermatrix for phylogenomic analyses.

278 We implemented the maximum likelihood approach using RAxML-HPC V.8 [61] with
279 a GTRGAMMA substitution model for each gene and a rapid bootstrap analysis with 500
280 replications. Then we filtered the bipartition trees that had $\geq 20\%$ support using Newick
281 utilities [62]. The resulting trees were rooted using phyx v1.2.1 [63], setting *Uncarina*
282 *grandidieri* (Baill.) Stapf (Lamiales) as the root. To estimate the species tree from the gene
283 trees, we used the coalescent approach with ASTRAL 5.6.1 to calculate the quartet scores,
284 which is the number of quartet trees present in the gene trees that are also present in the species
285 tree. Q1 shows the support of the gene trees for the main topology, q2 shows the support for
286 the first alternative topology, and q3 shows the support for the second alternative topology
287 [64]. We incorporated these scores into the species tree with an R script [65]. All trees were
288 visualized with FigTree v.1.4.4 [66].

289 In the nuclear phylogenomic tree resulting from the 353 low copy nuclear genes (Fig.
290 3), *C. pubescens* clusters within the Cinchonoideae, which is more closely related with the
291 Ixoroideae group than with Rubioideae. Most nodes are highly supported by quartet scores,
292 showing that a large proportion of the gene trees agreed with the species tree.

293 For the plastid phylogeny, we used *Sesamum indicum* L. as an outgroup from the
294 Lamiids cluster [67]. We performed maximum likelihood using the complete plastid genomes
295 of the 20 species available to date in the Gentianales. All the plastid genomes we analysed had
296 the classic quadripartite genomic structure, although some Rubiaceae species show the
297 tripartite structure [68]. We aligned the 20 Gentianales (Supp. Tab. 3) plastid genomes with
298 MAFFT v7.427 using the default parameter settings to perform the multiple sequence
299 alignments. Then we estimated the phylogenetic tree with the maximum likelihood (ML)
300 approach using the GTRCAT model RAxML-HPC v.8. We conducted heuristic searches with

301 1000 bootstrap replicates (rapid bootstrapping and search for the best-scoring ML tree). Both
302 analyses were performed on the Cipres Science Gateway [69].

303 As with the nuclear tree, the plastid trees were also clustered at the subfamily level,
304 recovering the Cinchonoideae, Ixoroideae, and Rubioideae as natural groups, alongside the two
305 species belonging to Pedilaceae used as outgroups for the phylogenetic analysis. For the plastid
306 data, the vast majority of nodes were strongly supported (16 had 100% support and all but one
307 node had 100% support). However, we found *Gynochthodes nanlingensis* (Y.Z.Ruan) Razafim.
308 & B.Bremer (Rubioideae) to cluster with other Apocynaceae species. While the same result
309 has previously been reported in other studies [70,71], it seems to be due to an erroneous DNA
310 sequence attributed to *G. nanlingensis* or a misidentification of the voucher, so it is
311 recommended this is thoroughly checked. Additionally, the ingroup showed that the
312 Cinchonoideae and Ixoroideae subfamilies are sisters and form a clade while Rubioideae is
313 placed as sister to this clade.

314 The placement of *C. pubescens* in the Cinchonoideae subfamily cluster using both the
315 plastid and nuclear data presented in this study is consistent with previous taxonomic and
316 phylogenetic studies [72] and gives support to the robustness of the assembled nuclear and
317 plastid genomes. As potential future work, the Nanopore sequencing data could be re-base
318 called using the latest algorithms from Oxford Nanopore to take advantage of recent
319 developments in this area over the last few years which has seen continuous improvement in
320 raw-read accuracy [73,74].

321

322 **2. Conclusion**

323 Using a combination of extensive short and long-read DNA datasets, we deliver the
324 first highly contiguous and robust nuclear and plastid genome assemblies for one of the
325 historically most traded and economically important *Cinchona* species, *C. pubescens*. The

326 abundant genomic resources provided here open up new research avenues to disentangle the
327 evolutionary history of the Fever tree.

328 In the short term, these genomic tools will significantly help to identify the genes
329 involved in the biosynthetic pathways of quinine alkaloids synthesis, identify the underpinning
330 genetic diversity of these genes both between and within species, and open doors on how the
331 expression of these genes is regulated. Our nuclear scaffold-level and plastid genome assembly
332 will enable future reference-guided assemblies, variant calling, and gene annotation to enhance
333 functional analysis within the *Cinchona* genus, with the potential to further explore the quinine
334 alkaloid biosynthetic pathway in-depth and hence enhance its potential for finding new
335 medicinal leads to treat malaria.

336

337 **Data availability**

338 The genome sequence data, and nuclear and plastid assemblies are available at the NBI
339 repository, under the BioProject number PRJNA768351.

340

341 **Competing interests**

342 The authors declare that they have no competing interests.

343

344 **Funding**

345 NR, AA, CB, and NC received funding from H2020 MSCA-ITN-ETN Plant.ID, a European
346 Union's Horizon 2020 research and innovation programme under grant agreement No 765000.
347 OAPE acknowledges financial support from the Swiss Orchid Foundation and the Lady
348 Sainsbury Fellowship at the Royal Botanic Gardens, Kew. PromethION sequencing (flow cells
349 and consumables) were provided by Oxford Nanopore Technologies. AA and NR acknowledge

350 funding from the SciLifeLab 2015 Biodiversity Program. AA is further funded by the Swedish
351 Research Council and the Royal Botanic Gardens, Kew.

352

353 **Author contributions**

354 IJL, OAPE, NR, MT and AA conceived the study. MN and OAPE collected plant tissue.
355 OAPE, IJL, RFP, MT and AA generated datasets. OAPE, NC, CK and MT conducted in-silico
356 analyses. NC and OAPE wrote the manuscript, with contributions from all co-authors.

357

358 **Acknowledgements**

359 We thank Jonathan Pugh, Vania Costa, and Simon Mayes for support and assistance during
360 Nanopore sequencing preparation and Claes Persson for taxonomic advice. Two anonymous
361 reviewers and the associate editor provided constructive feedback to this manuscript.

362 **Legends**

363 **Figure 1.** A. *Cinchona* trees in the Andean cloud forest. B. The *C. pubescens* specimen studied
364 in this work (CP9014) growing in the Temperate House at the Royal Botanic Gardens, Kew,
365 UK. C. Inflorescence of *C. pubescens*, CP9014. D. *Cinchona* barks from the Economic Botany
366 Collection, Kew, UK. E. Distribution map of the *Cinchona* genus across the American
367 continent shown in blue dots, modified from Maldonado et al. 2015 [75].

368

369 **Figure 2.** Annotated *C. pubescens* plastome. Genes displayed on the inside of the circle are
370 transcribed clockwise, while genes positioned on the outside are transcribed counter clockwise.

371

372 **Figure 3.** A. The coalescent-based species tree estimation of the Gentianales order is inferred
373 from low copy nuclear gene trees. Pie charts positioned on the nodes represent the percentage
374 of the gene tree quartets that agree with the topology of the main species tree (blue) and the

375 other two alternative gene tree quartets (orange: second child [R], sister group [S] | first child
376 [L], any other branch [O]; and grey: RO|LS). The genomic data of *Cinchona pubescens*
377 terminal marked with “*” was newly produced in this study. **B.** Phylogenetic tree showing the
378 relationships of twenty Gentianales species built from the whole plastid genome. Unless
379 shown, numbers on the branches represent Likelihood Bootstrap Percentages of 100. The
380 coloured boxes indicate the subfamily/family that sampled terminals belong to. Allele
381 frequencies for the fourth most common alleles, derived from reads mapped against the
382 scaffolds “utg230” (C) and “utg2” (D). Note that frequency distributions of the first and second
383 most frequent alleles are either skewed towards 0 or 1, denoting homozygote variants, and 0.5,
384 denoting heterozygote, diploid variants. (Inset): Frontal (left) and lateral view (right) of the
385 sequenced specimen (ID 1977-69) of *Cinchona pubescens* (photos: O. A. Pérez-Escobar).

386

387 **Table 1.** Summary table for the Illumina WGS and RNA-Seq libraries.

388 **Table 2.** Summary assembly statistics for *C. pubescens* using SMARTdenovo and RACON.

389 **Table 3.** Annotation metrics summary statistics for the nuclear annotation of *C. pubescens*.

390 **Additional files**

391 Supplementary Table 1. Summary statistics of the Nanopore reads.

392 Supplementary Table 2. Overview of the samples from the Tree of Life Explorer (Royal
393 Botanic Gardens, Kew) that were used in the phylogenetic analysis to construct the coalescent
394 tree.

395 Supplementary Table 3. Sample overview of the specimens and their accession numbers used
396 to infer the phylogenetic tree built using plastid data.

397 Supplementary figure 1. Plastid genome visualization of junctions IRb-SSC (*ycf1*) and LSC-
398 IRb (*rsp3*).

399

400

401 **References**

402 1. Pérez-Escobar OA, Zizka A, Bermúdez MA, Meseguer AS, Condamine FL, Hoorn C, et al.. The
403 Andes through time: evolution and distribution of Andean floras. *Trends Plant Sci.* 27:364–782022;

404 2. Gori B, Ulian T, Bernal HY, Diazgranados M. Understanding the diversity and biogeography of
405 Colombian edible plants. *Sci Rep.* 12:78352022;

406 3. Andersson L. A revision of the genus Cinchona (Rubiaceae-Cinchoneae). *Memoirs-New York*
407 *botanical garden.* NYBG NEW YORK BOTANICAL GARDEN; 1998;

408 4. Maldonado C, Persson C, Alban J, Antonelli A, Rønsted N. Cinchona anderssonii (Rubiaceae), a
409 new overlooked species from Bolivia. *Phytotaxa.* Magnolia Press; :203–82017;

410 5. Steere WC. The Cinchona-Bark Industry of South America. *Sci Mon.* American Association for the
411 Advancement of Science; 61:114–261945;

412 6. Kacprzak KM. Chemistry and biology of Cinchona alkaloids. *Nat Products Bioprospect.* Springer-
413 Verlag: Berlin; :605–412013;

414 7. Lee MR. Plants against malaria. Part 1: Cinchona or the Peruvian bark. *J R Coll Physicians Edinb.*
415 32:189–962002;

416 8. Walker K, Nesbitt M. Just the Tonic: A Natural History of Tonic Water. Kew Publishing;

417 9. : Home - Nucleotide - NCBI. <https://www.ncbi.nlm.nih.gov/nuccore> Accessed 2021 May 17.

418 10. Andersson L, Antonelli A. Phylogeny of the Tribe Cinchoneae (Rubiaceae), Its Position in
419 Cinchonoideae, and Description of a New Genus, Ciliosemina. *Taxon.* International Association for
420 Plant Taxonomy (IAPT); 54:17–282005;

421 11. Manns U, Bremer B. Towards a better understanding of intertribal relationships and stable tribal
422 delimitations within Cinchonoideae s.s. (Rubiaceae). *Mol Phylogenet Evol.* 56:21–392010;

423 12. Antonelli A, Clarkson JJ, Kainulainen K, Maurin O, Brewer GE, Davis AP, et al.. Settling a
424 family feud: a high-level phylogenomic framework for the Gentianales based on 353 nuclear genes
425 and partial plastomes. *Am J Bot.* 108:1143–652021;

426 13. Rusby HH. The Genus Cinchona in Bolivia. Bulletin of the Torrey Botanical Club.

427 14. Council OFE. European pharmacopoeia. v. 1. *Strasbourg, France: Council of Europe.* 2016;

428 15. Eyal S. The Fever Tree: from Malaria to Neurological Diseases. *Toxins.* 2018; doi:
429 10.3390/toxins10120491.

430 16. . IUCN Red List of threatened species. *Choice.* American Library Association; 43:43–2185 – 43–
431 21852005;

432 17. Jäger H, Tye A, Kowarik I. Tree invasion in naturally treeless environments: Impacts of quinine
433 (Cinchona pubescens) trees on native vegetation in Galápagos. *Biol Conserv.* Elsevier; 140:297–
434 3072007;

435 18. Sullivan DJ. Cinchona Alkaloids: Quinine and Quinidine. In: Staines HM, Krishna S, editors.
436 *Treatment and Prevention of Malaria: Antimalarial Drug Chemistry, Action and Use.* Basel: Springer

437 Basel; p. 45–68.

438 19. Renner SS, Wu S, Pérez-Escobar OA, Silber MV, Fei Z, Chomicki G. A chromosome-level
439 genome of a Kordofan melon illuminates the origin of domesticated watermelons. *Proc Natl Acad Sci
440 U S A*. 2021; doi: 10.1073/pnas.2101486118.

441 20. Al-Mssallem IS, Hu S, Zhang X, Lin Q, Liu W, Tan J, et al.. Genome sequence of the date palm
442 Phoenix dactylifera L. *Nat Commun.* 4:22742013;

443 21. Shukla VK, Doyon Y, Miller JC, DeKelver RC, Moehle EA, Worden SE, et al.. Precise genome
444 modification in the crop species Zea mays using zinc-finger nucleases. *Nature*. 459:437–412009;

445 22. Lau KH, Bhat WW, Hamilton JP, Wood JC, Vaillancourt B, Wiegert-Rininger K, et al.. Genome
446 assembly of Chiococca alba uncovers key enzymes involved in the biosynthesis of unusual
447 terpenoids. *DNA Res.* Oxford Academic; 2020; doi: 10.1093/dnares/dsaa013.

448 23. Denoeud F, Carretero-Paulet L, Dereeper A, Droc G, Guyot R, Pietrella M, et al.. The coffee
449 genome provides insight into the convergent evolution of caffeine biosynthesis. *Science*. 345:1181–
450 42014;

451 24. Tran HTM, Ramaraj T, Furtado A, Lee LS, Henry RJ. Use of a draft genome of coffee (*Coffea
452 arabica*) to identify SNPs associated with caffeine content. *Plant Biotechnol J.* 16:1756–662018;

453 25. Park J, Kim Y, Xi H, Heo K-I. The complete chloroplast genome of coffee tree, *Coffea arabica* L.
454 “Blue Mountain” (Rubiaceae). *Mitochondrial DNA Part B*. Taylor & Francis; 4:2436–72019;

455 26. : London Calling: Live first-time sequencing of the Fever Tree - the plant that some say has saved
456 millions of lives from malaria. [https://nanoporetech.com/about-us/news/london-calling-live-first-time-
sequencing-fever-tree-plant-some-say-has-saved](https://nanoporetech.com/about-us/news/london-calling-live-first-time-
457 sequencing-fever-tree-plant-some-say-has-saved) Accessed 2021 Jul 8.

458 27. Doležel J, Kubaláková M, Suchánková P, Kovářová P, Bartoš J, Šimková H. Chromosome
459 Analysis and Sorting. Flow Cytometry with Plant Cells.

460 28. Pellicer J, Powell RF, Leitch IJ. The Application of Flow Cytometry for Estimating Genome Size,
461 Ploidy Level Endopolyploidy, and Reproductive Modes in Plants. *Methods Mol Biol.* 2222:325–
462 612021;

463 29. Loureiro J, Rodriguez E, Doležel J, Santos C. Two New Nuclear Isolation Buffers for Plant DNA
464 Flow Cytometry: A Test with 37 Species. *Ann Bot*. Oxford University Press; 100:8752007;

465 30. Bennett MD, Smith JB. Nuclear dna amounts in angiosperms. *Philos Trans R Soc Lond B Biol Sci.*
466 274:227–741976;

467 31. Marçais, Kingsford. JELLYFISH–fast, parallel k-mer counting for DNA. *Bioinformatics*.

468 32. Verture GW, Sedlazeck FJ, Nattestad M, Underwood CJ, Fang H, Gurtowski J, et al..
469 GenomeScope: fast reference-free genome profiling from short reads. *Bioinformatics*. 33:2202–
470 42017;

471 33. Andrews S, Others. FastQC: a quality control tool for high throughput sequence data. Babraham
472 Bioinformatics, Babraham Institute, Cambridge, United Kingdom;

473 34. Schubert M, Lindgreen S, Orlando L. AdapterRemoval v2: rapid adapter trimming, identification,
474 and read merging. *BMC Res Notes*. 9:882016;

475 35. : MPI-MP CHLOROBOX - GeSeq. <https://chlorobox.mpimp-golm.mpg.de/geseq.html> Accessed
476 2021 May 18.

477 36. Tillich M, Lehwerk P, Pellizzer T, Ulbricht-Jones ES, Fischer A, Bock R, et al.. GeSeq - versatile
478 and accurate annotation of organelle genomes. *Nucleic Acids Res.* 45:W6–112017;

479 37. Lowe TM, Eddy SR. tRNAscan-SE: a program for improved detection of transfer RNA genes in
480 genomic sequence. *Nucleic Acids Res.* 25:955–641997;

481 38. Laslett D, Canback B. ARAGORN, a program to detect tRNA genes and tmRNA genes in
482 nucleotide sequences. *Nucleic Acids Res.* 32:11–62004;

483 39. Greiner S, Lehwerk P, Bock R. OrganellarGenomeDRAW (OGDRAW) version 1.3.1: expanded
484 toolkit for the graphical visualization of organellar genomes. *Nucleic Acids Res.* 47:W59–642019;

485 40. Schubert M, Ermini L, Sarkissian CD, Jónsson H, Ginolhac A, Schaefer R, et al.. Characterization
486 of ancient and modern genomes by SNP detection and phylogenomic and metagenomic analysis using
487 PALEOMIX. *Nature Protocols*.

488 41. Li H, Durbin R. Fast and accurate short read alignment with Burrows-Wheeler transform.
489 *Bioinformatics*. 25:1754–602009;

490 42. De Coster W. NanoPlot. Github;

491 43. Koren S, Walenz BP, Berlin K, Miller JR, Bergman NH, Phillippy AM. Canu: scalable and
492 accurate long-read assembly via adaptive k-mer weighting and repeat separation. *Genome Res.*
493 27:722–362017;

494 44. Ruan J. SMARTdenovo: Ultra-fast de novo assembler using long noisy reads. *Github Available
495 at: <https://github.com/ruanjue/smardenovo> [Accessed January 10, 2019]*. 2018;

496 45. Vaser R, Sović I, Nagarajan N, Šikić M. Fast and accurate de novo genome assembly from long
497 uncorrected reads. *Genome Res.* 27:737–462017;

498 46. Li H. Minimap2: pairwise alignment for nucleotide sequences. *Bioinformatics*. 34:3094–1002018;

499 47. Li H, Handsaker B, Wysoker A, Fennell T, Ruan J, Homer N, et al.. The Sequence
500 Alignment/Map format and SAMtools. *Bioinformatics*. 25:2078–92009;

501 48. Simão FA, Waterhouse RM, Ioannidis P, Kriventseva EV, Zdobnov EM. BUSCO: assessing
502 genome assembly and annotation completeness with single-copy orthologs. *Bioinformatics*. 31:3210–
503 22015;

504 49. Augusto Corrêa Dos Santos R, Goldman GH, Riaño-Pachón DM. ploidyNGS: visually exploring
505 ploidy with Next Generation Sequencing data. *Bioinformatics*. 33:2575–62017;

506 50. Grabherr MG, Haas BJ, Yassour M, Levin JZ, Thompson DA, Amit I, et al.. Full-length
507 transcriptome assembly from RNA-Seq data without a reference genome. *Nat Biotechnol.* 29:644–
508 522011;

509 51. Dobin A, Davis CA, Schlesinger F, Drenkow J, Zaleski C, Jha S, et al.. STAR: ultrafast universal
510 RNA-seq aligner. *Bioinformatics*. 29:15–212013;

511 52. Haas BJ, Delcher AL, Mount SM, Wortman JR, Smith RK Jr, Hannick LI, et al.. Improving the
512 Arabidopsis genome annotation using maximal transcript alignment assemblies. *Nucleic Acids Res.*
513 31:5654–662003;

514 53. Stanke M, Keller O, Gunduz I, Hayes A, Waack S, Morgenstern B. AUGUSTUS: ab initio
515 prediction of alternative transcripts. *Nucleic Acids Res.* 34:W435–92006;

516 54. Kent WJ. BLAT—The BLAST-Like Alignment Tool. *Genome Res.* 12:656–642002;

517 55. Manchanda N, Portwood JL 2nd, Woodhouse MR, Seetharam AS, Lawrence-Dill CJ, Andorf CM,
518 et al.. GenomeQC: a quality assessment tool for genome assemblies and gene structure annotations.
519 *BMC Genomics.* 21:1932020;

520 56. Baker WJ, Bailey P, Barber V, Barker A, Bellot S, Bishop D, et al.. A Comprehensive
521 Phylogenomic Platform for Exploring the Angiosperm Tree of Life. *Syst Biol.* 2021; doi:
522 10.1093/sysbio/syab035.

523 57. : Index of /pub/paftol. <http://sftp.kew.org/pub/paftol/> Accessed 2021 May 19.

524 58. Johnson MG, Gardner EM, Liu Y, Medina R, Goffinet B, Shaw AJ, et al.. HybPiper: Extracting
525 coding sequence and introns for phylogenetics from high-throughput sequencing reads using target
526 enrichment. *Appl Plant Sci.* Wiley; 4:16000162016;

527 59. Li H. seqtk Toolkit for processing sequences in FASTA/Q formats. *GitHub.* 767:692012;

528 60. Katoh K, Kuma K-I, Toh H, Miyata T. MAFFT version 5: improvement in accuracy of multiple
529 sequence alignment. *Nucleic Acids Res.* 33:511–82005;

530 61. Stamatakis A. RAxML version 8: a tool for phylogenetic analysis and post-analysis of large
531 phylogenies. *Bioinformatics.* 30:1312–32014;

532 62. Junier T, Zdobnov EM. The Newick utilities: high-throughput phylogenetic tree processing in the
533 UNIX shell. *Bioinformatics.* 26:1669–702010;

534 63. Brown JW, Walker JF, Smith SA. Phyx: phylogenetic tools for unix. *Bioinformatics.* 33:1886–
535 82017;

536 64. Zhang C, Rabiee M, Sayyari E, Mirarab S. ASTRAL-III: polynomial time species tree
537 reconstruction from partially resolved gene trees. *BMC Bioinformatics.* 19:1532018;

538 65. Bellot S. scripts. Github;

539 66. Rambaut A. FigTree v1. 4.

540 67. Yi D-K, Kim K-J. Complete chloroplast genome sequences of important oilseed crop Sesamum
541 indicum L. *PLoS One.* 7:e358722012;

542 68. Ly SN, Garavito A, De Block P, Asselman P, Guyeux C, Charr J-C, et al.. Chloroplast genomes of
543 Rubiaceae: Comparative genomics and molecular phylogeny in subfamily Ixoroideae. *PLoS One.*
544 15:e02322952020;

545 69. Miller MA, Pfeiffer W, Schwartz T. The CIPRES science gateway: a community resource for
546 phylogenetic analyses. *Proceedings of the 2011 TeraGrid Conference: Extreme Digital Discovery.*
547 New York, NY, USA: Association for Computing Machinery; p. 1–8.

548 70. Zhou T, Wang J, Jia Y, Li W, Xu F, Wang X. Comparative Chloroplast Genome Analyses of
549 Species in Gentiana section Crucifera (Gentianaceae) and the Development of Authentication Markers.
550 *Int J Mol Sci.* 2018; doi: 10.3390/ijms19071962.

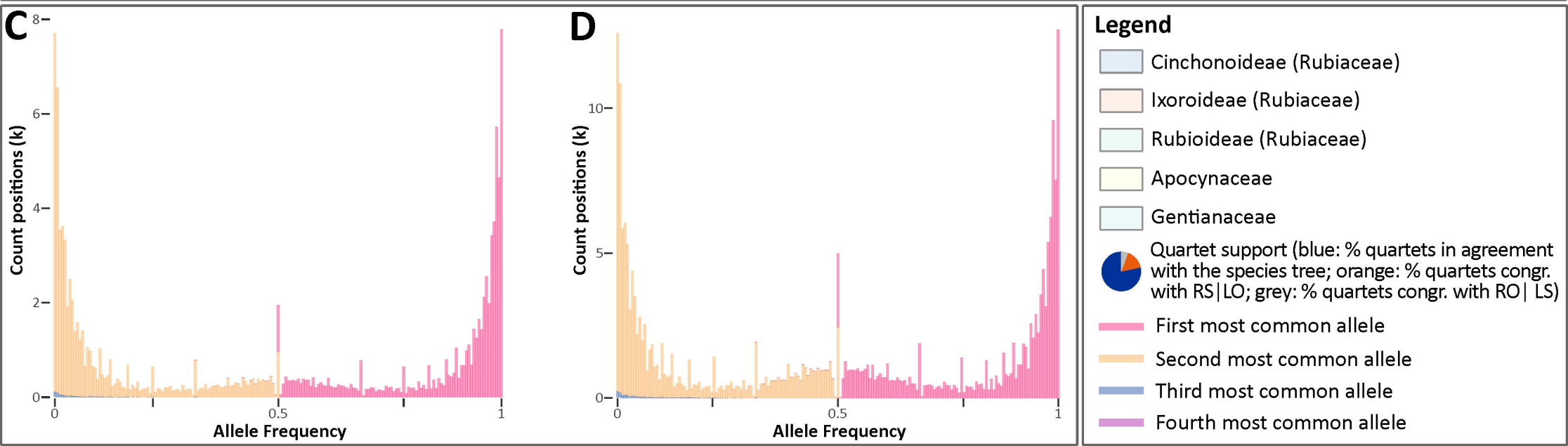
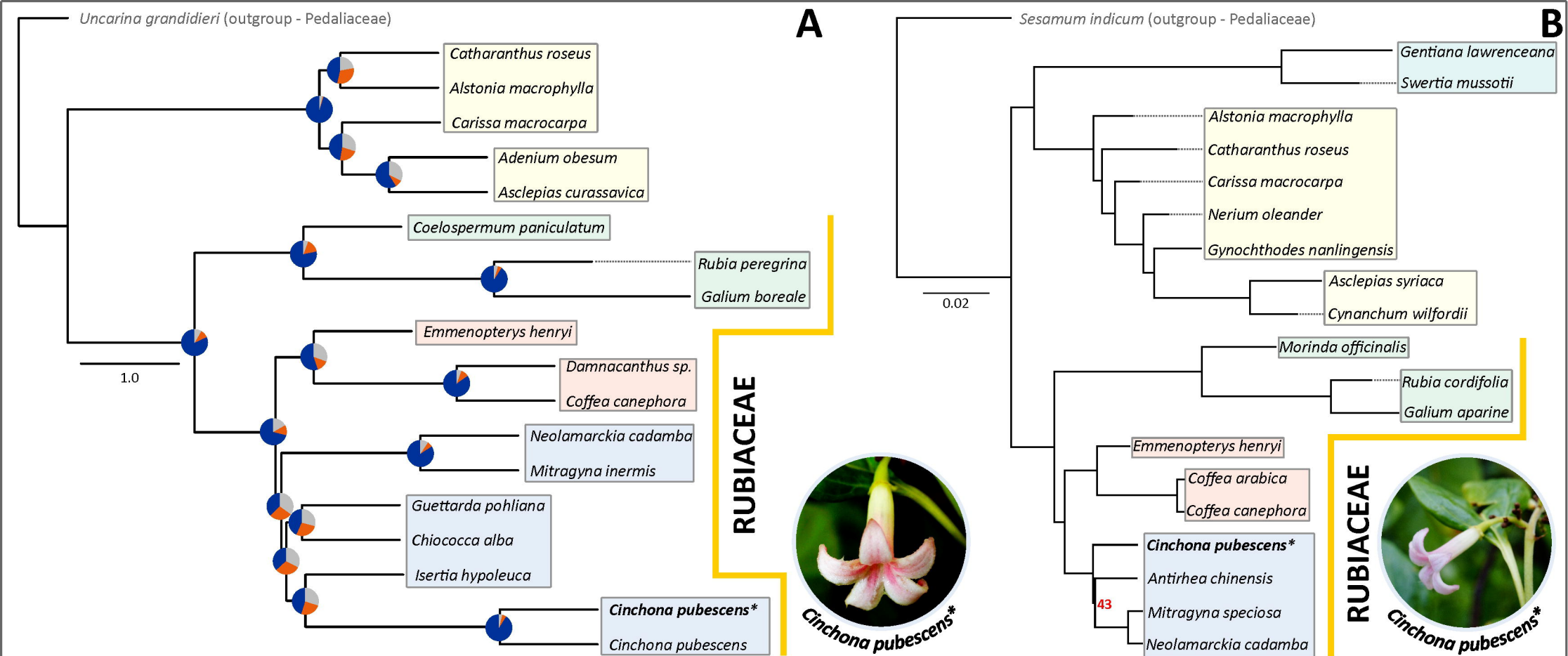
551 71. Zhang Y, Zhang J-W, Yang Y, Li X-N. Structural and Comparative Analysis of the Complete
552 Chloroplast Genome of a Mangrove Plant: Scyphiphora hydrophyllacea Gaertn. f. and Related
553 Rubiaceae Species. *For Trees Livelihoods.* Multidisciplinary Digital Publishing Institute;
554 10:10002019;

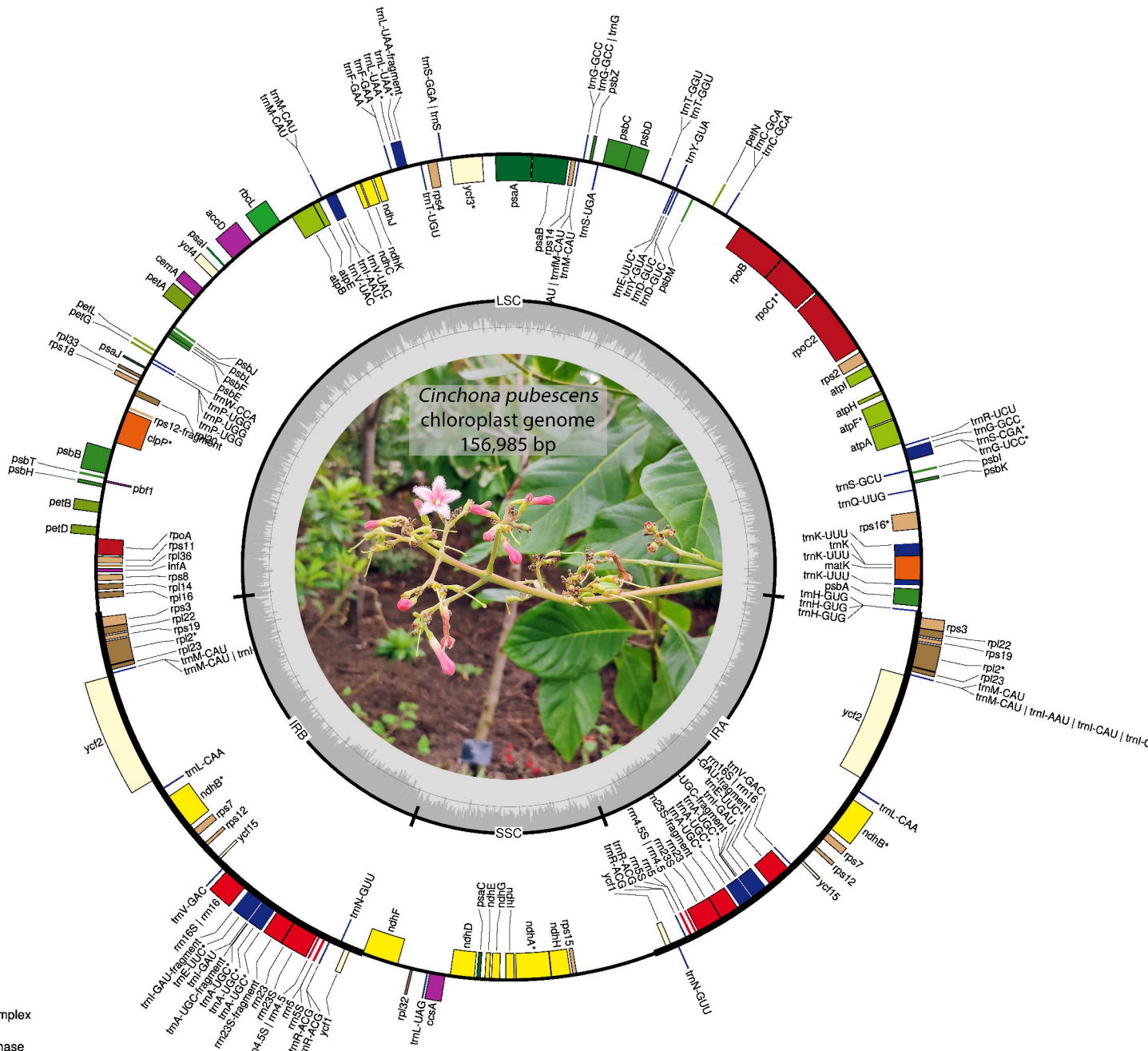
555 72. Robbrecht E, Manen J-F. The Major Evolutionary Lineages of the Coffee Family (Rubiaceae,
556 Angiosperms). Combined Analysis (nDNA and cpDNA) to Infer the Position of Coptosapelta and
557 Luculia, and Supertree Construction Based on rbcL, rps16, trnL-trnF and atpB-rbcL Data. A New
558 Classification in Two Subfamilies, Cinchonoideae and Rubioideae. *Syst Geogr Plants*. National
559 Botanic Garden of Belgium; 76:85–1452006;

560 73. LaPierre N, Egan R, Wang W, Wang Z. De novo Nanopore read quality improvement using deep
561 learning. *BMC Bioinformatics*. 20:5522019;

562 74. Chen Y, Nie F, Xie S-Q, Zheng Y-F, Dai Q, Bray T, et al.. Efficient assembly of nanopore reads
563 via highly accurate and intact error correction. *Nat Commun*. 12:602021;

564 75. Maldonado C, Molina CI, Zizka A, Persson C, Taylor CM, Albán J, et al.. Estimating species
565 diversity and distribution in the era of Big Data: to what extent can we trust public databases? *Glob
566 Ecol Biogeogr*. 24:973–842015;





- photosystem I
- photosystem II
- cytochrome b/f complex
- ATP synthase
- NADH dehydrogenase
- RubisCO large subunit
- RNA polymerase
- ribosomal proteins (SSU)
- ribosomal proteins (LSU)
- clpP, matK
- other genes
- hypothetical chloroplast reading frames (ycf)
- transfer RNAs
- ribosomal RNAs

biosample_accession	Library_ID	Tissue	Source	Technology	Total Number of		
					Yield (Gb)	reads (million)	%GC
SAMN22031859	CP9014LG	Leave	Genomic	Illumina HiSeq X	128.4	428	42
SAMN22031859	CP9014L	Leave	Transcriptomic	Illumina HiSeq X	38	101.6	42
SAMN22031859	CP9014YL	Young leaf	Transcriptomic	Illumina HiSeq X	32.6	87.1	46
SAMN22031859	CP9014LB	Leaf bud	Transcriptomic	Illumina HiSeq X	NA	NA	NA
SAMN22031859	CP9014Y	Young bract	Transcriptomic	Illumina HiSeq X	NA	NA	NA
SAMN22031859	CP9014B	Mature bract	Transcriptomic	Illumina HiSeq X	10.3	83.32	42
SAMN22031859	CP9014F	Flower in anthesis	Transcriptomic	Illumina HiSeq X	17.3	93.28	43
SAMN22031859	CP9014FBO	Flower bud - older	Transcriptomic	Illumina HiSeq X	18.6	127.9	43
SAMN22031859	CP9014FB	Flower bud - young	Transcriptomic	Illumina HiSeq X	17.9	103.8	43

	SMARTdenovo	RACON
Size_includeN	903037179	9.04E+08
Size_withoutN	903037179	9.04E+08
Seq_Num	603	603
Mean_Size	1497574	1499914
Median_Size	801066	802662
Longest_Seq	14628764	14747124
Shortest_Seq	33171	25882
GC_Content (%)	33.17	33.07
N50	2783363	2802128
L50	93	92
N90	682446	684435
Gap (%)	0	0

Number of gene models	72305
Minimum gene length	275
Maximum gene length	65857
Average gene length	4579.5
Number of exons	339698
Average number of exons per gene model	4.7
Average exon length	298.3
Number of transcripts	72305
Average number of transcripts per gene model	1
Number of gene models less than 200bp length	0